

GUST LOADING FACTOR: NEW MODEL

By Yin Zhou¹ and Ahsan Kareem,² Member, ASCE

ABSTRACT: Wind loads on structures under the buffeting action of wind gusts have traditionally been treated by the “gust loading factor” (GLF) method in most major codes and standards around the world. In this scheme, the equivalent static wind loading used for design is equal to the mean wind force multiplied by the GLF. Although the traditional GLF method ensures an accurate estimation of the displacement response, it may fall short in providing a reliable estimate of other response components. To overcome this shortcoming, a more realistic procedure for determining design loads on tall structures is proposed. This paper highlights the new model, in which the GLF is based on the base bending moment rather than the displacement. The expected extreme base moment is computed by multiplying the mean base moment by the proposed GLF. The base moment is then distributed to each floor in terms of the floor load in a format that is very similar to the one used to distribute the base shear in earthquake engineering practice. In addition, a simple relationship between the proposed base moment GLF and the traditional GLF is derived, which makes it convenient to employ the proposed approach while utilizing the existing background information. Numerical examples are presented to demonstrate the efficacy of the proposed procedure in light of the traditional approach.

INTRODUCTION

The diversity of structures that are sensitive to the effects of wind and the increasing need to improve the performance of constructed facilities have placed a growing importance on the problem of wind effects on structures. Typically, structures are designed based on the recommended equivalent static wind loading (ESWL) given in codes and standards. Currently, the ESWL in building codes is estimated based on the “gust loading factor” (GLF) approach proposed by Davenport (1967). According to the GLF method, the ESWL is equal to the mean wind force multiplied by a GLF. The GLF accounts for the dynamics of wind fluctuations and any load amplification introduced by the building dynamics. Since its introduction, several formulations of the GLF have been advanced; details can be found in Simiu and Scanlan (1996). Because of its simplicity, the GLF method has received a widespread acceptance around the world and is employed in wind load codes and standards in almost all major countries [e.g., EUROCODE (1995), AIJ (1996), NRCC (1996), ASCE (1999)]. It should be pointed out that the Australian Standard (1989) and the ACI standard (1988) use the GLF for the base bending moment (BBM); however, the GLF is based on the traditional definition.

Despite its many advantages, it is noted that the current GLF method has its shortcoming in the application of this method for relatively long, tall, and flexible structures. Although the gust factor was originally defined for any load effect, it is actually based on the displacement response; i.e., the gust factor is essentially the ratio between the extreme and the mean displacement response and is referred to as DGLF in the subsequent discussion. The DGLF is used indiscriminately for any response component in practice, which may yield inaccurate estimates. Because only the fluctuating and mean displacement responses in the first mode are included in the derivation, the DGLF is constant for a given structure. When the constant DGLF is used for estimating the extreme ESWL following the

line of the conventional GLF or DGLF approach, an ESWL with the same distribution as that of the mean wind load is obtained. This contradicts the common understanding of the ESWL on tall, long, and flexible structures. For this type of structure, the resonant response is the dominant one. Therefore, the distribution of the ESWL should depend on the structural mass distribution and mode shape. Zhou et al. (1999a,b) have noted that the DGLF method provides an accurate assessment of the structural displacement, but results in less accurate estimation of other response quantities, such as the base shear force.

Using influence functions, Davenport (1999) and Drybre and Hansen (1997) have developed a revised GLF concept or procedure that is based on the response related to the influence function, but not limited to the displacement. This is certainly an improvement, since these procedures would ensure an accurate estimation of the response involved. However, the response-specific GLF also has its own shortcoming, since each response component requires a separate GLF. For engineering applications, this is inconvenient and can be arbitrarily tedious, since the response components of engineering interest are various.

Realizing the special role that the ESWL plays in wind engineering, Zhou et al. (2000) proposed a theoretical formulation for the equivalent static buffeting wind loads on structures. The rigorous description of the ESWL can be used to reduce the shortcomings of the current approach for design.

This paper presents a new model for the along-wind ESWL on tall structures. The model employs a GLF associated with the BBM, referred to as the MGLF in the subsequent discussion. The expected extreme BBM is computed by multiplying the mean BBM by the MGLF. The base moment is then distributed to other floors. Furthermore, a simple relationship between the proposed MGLF and the traditional DGLF is established, which enables utilization of the existing procedures for DGLF available in codes and standards in the proposed scheme. A numerical example is presented to demonstrate the efficacy of the proposed procedure.

BACKGROUND

For the sake of comparison and completeness, the traditional DGLF approach is briefly outlined here. In the DGLF approach, the peak load is given by

$$\hat{P}(z) = G \cdot \bar{P}(z) \quad (1)$$

where G = gust factor, which takes into account the dynamics of gusts and the structure; and $\bar{P}(z)$ = mean wind force.

¹Postdoctoral Res. Assoc., NatHaz Modeling Lab., Dept. of Civ. Engrg. and Geological Sci., Univ. of Notre Dame, Notre Dame, IN 46556. E-mail: yzhou@nd.edu

²Robert M. Moran Prof. and Chair, NatHaz Modeling Lab., Dept. of Civ. Engrg. and Geological Sci., Univ. of Notre Dame, Notre Dame.

Note. Associate Editor: Timothy Reinhold. Discussion open until July 1, 2001. To extend the closing date one month, a written request must be filed with the ASCE Manager of Journals. The manuscript for this paper was submitted for review and possible publication on February 8, 2000. This paper is part of the *Journal of Structural Engineering*, Vol. 127, No. 2, February, 2001. ©ASCE, ISSN 0733-9445/01/0002-0168-0175/\$8.00 + \$.50 per page. Paper No. 22254.

In the DGLF approach, G is evaluated in terms of the displacement response (Davenport 1967)

$$G_Y = \hat{Y}(z)/\bar{Y}(z) \quad (2)$$

where G_Y = DGLF; \bar{Y} = mean displacement; and \hat{Y} = expected extreme displacement response. For a stationary process, G_Y is given by

$$G_Y = 1 + g_Y \sigma_Y(z)/\bar{Y}(z) = 1 + 2g_Y I_H \sqrt{B + R} \quad (3)$$

in which g_Y = displacement peak factor; σ_Y = RMS displacement; B and R = background and resonant response factors, respectively; and $I_H = \sigma_u/\bar{U}_H$ = turbulent intensity evaluated at the top of the structure. The mean wind load is given by

$$\bar{P}(z) = 1/2\rho C_D W \bar{U}_H^2 (z/H)^{2\alpha} \quad (4)$$

in which ρ = air density; C_D = drag coefficient; W = width of the structure normal to the oncoming wind; $\bar{U}(z) = \bar{U}_H(z/H)^\alpha$ = mean wind velocity at height z above the ground, where \bar{U}_H = mean wind velocity evaluated at the top height of the structure, H ; and α = exponent of the mean wind velocity profile.

Alternatively, (3) can be expressed in terms of peak factors associated with the background and resonant response, as given in ASCE 7-98 (ASCE 1999)

$$G_Y = 1 + 2I_H \sqrt{g_u^2 \cdot B + g_R^2 \cdot R} \quad (5)$$

where g_u = wind velocity peak factor; and g_R = resonant peak factor. For a Gaussian process, $g_R = \sqrt{2 \ln(f_1 T) + 0.5772/\sqrt{2 \ln(f_1 T)}}$, in which T = observation time; and $R = SE/\zeta$, where S = size reduction factor, E = gust energy factor, and ζ = critical damping ratio of the first mode.

All traditional formulations of the DGLF are based on the preceding expressions, but differ in their modeling of turbulence and structural models. These details have led to variations in the prediction of gust factors derived from different DGLF formulations. A derivation of DGLF consistent with our formulation is given in Appendix I for the sake of completeness and convenient reference. The coefficients B , E , and S are provided graphically in some codes or in a closed form in others (Davenport 1967; Solari 1993a,b; Solari and Kareem 1998).

Eq. (5) can be rewritten in terms of mean, background, and resonant components, as

$$G_Y = 1 + \sqrt{G_{YB}^2 + G_{YR}^2} \quad (6)$$

where G_{YB} and G_{YR} = background and resonant components of the DGLF, respectively, and are given in Appendix I.

PROPOSED MGLF

Unlike the traditional DGLF approach, the proposed procedure uses a BBM-based GLF or MGLF, which is defined as

$$G_M = \hat{M}/\bar{M} \quad (7)$$

where G_M = MGLF; \bar{M} = mean BBM; and \hat{M} = expected extreme BBM response. Similar to the treatment of the DGLF, when considering a stationary Gaussian process, the MGLF can be computed by

$$G_M = 1 + g_M \sigma_M/\bar{M} \quad (8)$$

in which g_M = peak factor; and σ_M = RMS BBM response.

The BBM response includes the effects of turbulence-structure-interaction, which can be captured by the following equation:

$$m_1^* \ddot{\xi}_1(t) + c_1^* \dot{\xi}_1(t) + k_1^* \xi_1(t) = \bar{P}_1^*(t) \quad (9)$$

where m_1^* , c_1^* , k_1^* , \bar{P}_1^* , and ξ_1 = generalized mass, damping, stiffness, load, and displacement in the first mode, respectively.

An equivalent-static generalized wind load, $k_1^* \xi_1(t)$, can be obtained in terms of the generalized displacement. When this load is applied statically, the corresponding generalized displacement and any other response components are identical to those obtained from a complete dynamic analysis.

Accordingly, referring to (34) and (39) (Appendix I), the power spectral density (PSD) of the generalized equivalent-static wind load is given by

$$S_{\bar{P}_1^*}(f) = k_1^{*2} S_{\xi}(f) = S_{P_1}(f) |H_1(f)|^2 \quad (10)$$

in which the generalized equivalent-static wind load is $\bar{P}_1^*(t) = \int_0^H \bar{P}(z, t) \varphi_1(z) dz$, where $\bar{P}(z, t)$ = ESWL. Note that symbols used for the externally applied loads are utilized here for the ESWL and its associations, but are given in typewriter font to distinguish them from the externally applied loads.

The ESWL, $\bar{P}(z, t)$, is usually distributed, along the building height, in a manner that differs from the mean or fluctuating externally applied aerodynamic loads. Nonetheless, for a linear mode shape, the following relationships are valid for both the externally applied and the equivalent-static wind loads:

$$\bar{P}^* = \tilde{M}/H \quad (11)$$

$$\bar{P}_1^* = \tilde{M}/H \quad (12)$$

where \tilde{M} and \tilde{M} = fluctuating components of the externally applied and the induced BBMs, respectively. It is important to distinguish clearly between the equivalent-static/induced and the aerodynamic/externally-applied wind loads. The former includes any amplification resulting from building dynamics. Substituting (11) and (12) into (10) leads to

$$S_{\bar{P}_1^*}(f) = S_{\tilde{M}}(f) |H_1(f)|^2 \quad (13)$$

The preceding equation has also been referred to by Boggs and Peterka (1989) and Boggs (1991) in reference to the high frequency base balance (HFBB) technique.

Eq. (13) is utilized here to present a new probabilistic treatment of buffeting as highlighted in Fig. 1(b). Two advantages associated with this concept are: (1) it gives a very concise description of the relationship between the aerodynamic load and the induced wind load effects, which facilitates convenient evaluation of the ESWL; and (2) in the traditional formulation, the aerodynamic admittance function is difficult to ascertain from theoretical consideration and therefore has led to significant variability in the response estimates [e.g., Lee and Ng (1988), and Zhou and Kareem, in preparation, (2000)]. This can be attributed to a number of reasons including the role of the strip and quasi-steady theories (Kareem 1986). In the scheme shown in Fig. 1(a), the aerodynamic admittance is actually the transfer function between the input turbulence and the generalized wind load. The generalized wind load is arbitrary in magnitude depending on the normalization scheme used to define the mode shape, and in this format the aerodynamic admittance also becomes a function of the mode shape as shown in (36)–(38) (Appendix I). This complicates the verification of the theoretical formulation with experimental measurements. On the other hand, in the proposed formulation, the aerodynamic admittance function describes the relationship between the input turbulence and the BBM. The latter is realistic and can be ascertained conveniently using effective tools, such as the HFBB technique. Therefore, the existing aerodynamic wind load data can be used to aid in improving the accuracy of the current model. The availability of additional data can further refine the predictions based on this model (Zhou and Kareem, in preparation, 2000).

Rewrite (13) in the following nondimensional form:

$$\sigma_{\bar{P}_1^*}/\bar{M} = \left(\int_0^\infty S_{\tilde{M}}(f) |H_1(f)|^2 df \right)^{1/2} / \bar{M} \quad (14)$$

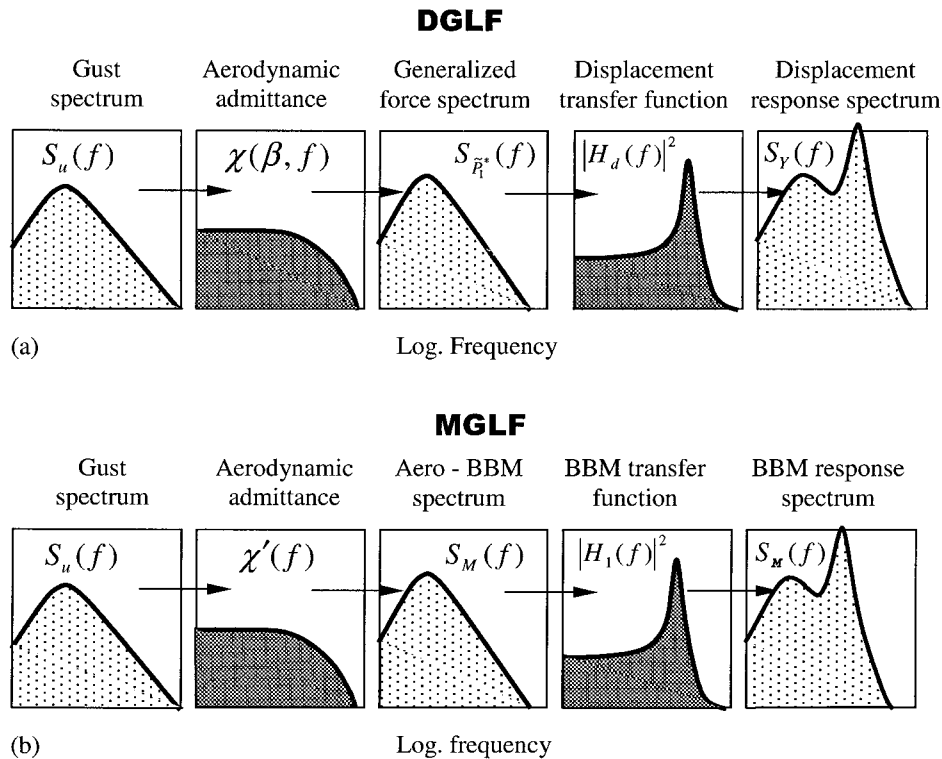


FIG. 1. Probabilistic-Dynamics Based Approaches to Gust Loading: (a) DGLF Model; (b) MGLF Model

Substituting (14) into (8) and after some mathematical manipulations, the MGLF is given by

$$G_M = 1 + 2I_H \sqrt{g_u^2 B + g_{RR}^2} = 1 + \sqrt{G_{MB}^2 + G_{MR}^2} \quad (15)$$

where $G_{MB} = 2I_H g_u \sqrt{B}$ and $G_{MR} = 2I_H g_{RR} \sqrt{R}$ = background and resonant components of the MGLF, respectively; and B and R = background and resonant response factors, respectively.

For code application of the MGLF, B and R can be obtained from graphs or closed-form expressions like the ones used in the DGLF. However, by employing the simple relationship between the DGLF and the MGLF, as described in the next section, the effort required to obtain the MGLF can be significantly reduced.

RELATIONSHIP BETWEEN MGLF AND DGLF

A comparison between (14) and (41) and the use of the relationships given in (11) and (12) provides the following relationship:

$$\sigma_{\bar{M}} / \bar{M} = \sigma_Y / \bar{Y} \quad (16)$$

Substituting (16) into (3) and (8) provides a very meaningful relationship

$$G_M = G_Y \quad (17)$$

This means effectively that the MGLF is numerically equal to the traditional DGLF, which is prescribed in the current codes and standards. This would aid in using the existing procedures in codes and standards for the evaluation of MGLF, thus providing a smooth transition from the currently established procedures to the proposed one.

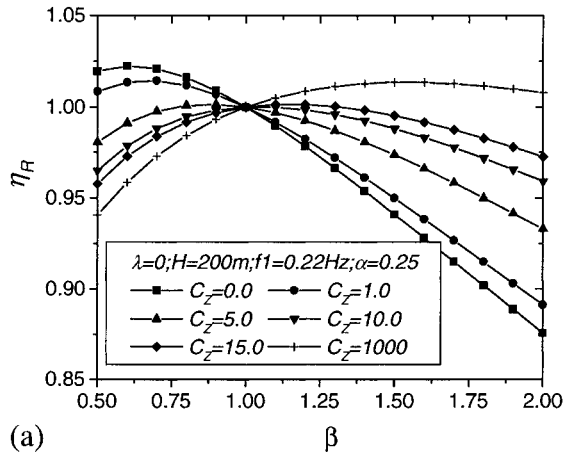
Nonetheless, the equivalence noted in (17) requires a linear mode shape. Some structures may exhibit a departure from the linear mode shape, which has been addressed by several researchers [e.g., Vickery (1970), Boggs and Peterka (1989), Zhou et al. (1999b), Zhou and Kareem, in preparation (2000)]. The influence of a nonlinear mode shape on the relationship between the MGLF and the DGLF is treated in the following section.

A detailed derivation of the MGLF along the lines of the DGLF formulation in Appendix I is given in Appendix II. As shown in this derivation, the background component of the MGLF is given by (48), which is identical to (44), which describes the background component of the DGLF. It is noteworthy that this result is consistent with (17). For the background response $|H_1(f)| = 1$, and the background BBM component is exactly the aerodynamic base moment, irrespective of the structural and turbulence characteristics as indicated in (10). Nonetheless, a similar relationship between the resonant components of the MGLF and the DGLF is not that straightforward. However, using (45) and (52), a deviation factor can be defined to relate the resonant component based on the two approaches

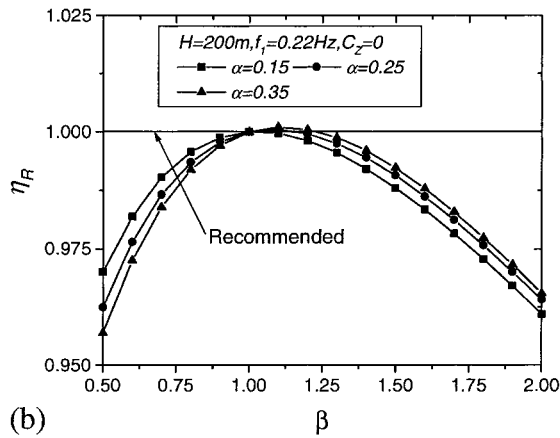
$$\eta_R = \frac{G_{MR}}{G_{YR}} = \frac{(1 + 2\beta)(2 + 2\beta)(2 + \alpha)}{(1 + \alpha + \beta)[(2 + 2\beta) - \lambda(1 + 2\beta)]} \frac{[(3 + \beta) - \lambda(2 + \beta)]}{(3 + \beta)(2 + \beta)} \cdot \sqrt{\frac{|J_z(\alpha, \beta, f_1)|^2}{|J_z(\alpha, 1, f_1)|^2}} \quad (18)$$

where α = wind velocity profile exponent; β = mode shape exponent in (31); λ = mass reduction parameter in (32); and J_z is defined in (38). As noted previously, for a linear mode shape, η_R is unity regardless of other parameters.

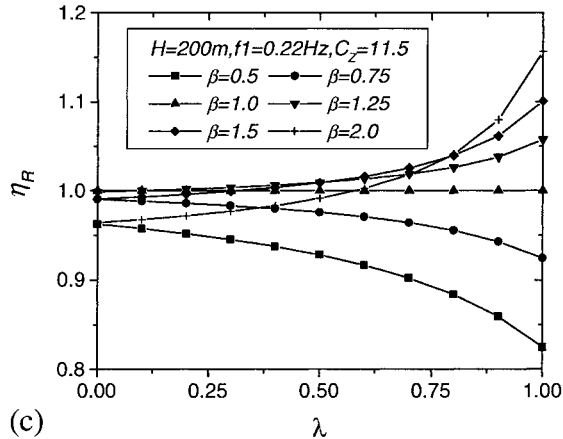
On the other hand, when the mode shape of the structure is nonlinear, the resonant deviation factor is dependent on both the structural and the turbulence characteristics. The effect of correlation of the approaching flow defined in (38) is illustrated in Fig. 2(a). Usually, there is a significant variation in the definition of this correlation function. However, for the two limiting correlation cases, i.e., $C_z = 0$ (fully correlated) and $C_z \rightarrow \infty$ (delta-correlated), the correlation effect is within 15% when $\beta = 2.0$. In the general range of $C_z = 5 \sim 15$, this effect is within 5% for $\beta = 0.5 \sim 2.0$. Fig. 2(b) shows the effect of a nonlinear mode shape on the resonant response deviation factor. Using $C_z = 11.5$ (Solari 1993a), the effect of a nonlinear mode shape is within 5% for $\beta = 0.5 \sim 2.0$, and the deviation factor is insensitive to the wind velocity exponent, α . The deviation factor is also insensitive to the mass reduction factor,



(a)



(b)



(c)

FIG. 2. Resonant Response Deviation Factor [Eq. (18)]

λ , which introduces an error of less than 3% when $\lambda \leq 0.5$, which is a reasonable value for most buildings. The effect of a non-uniform mass distribution is illustrated in Fig. 2(c).

The preceding parameter study shows that the deviation factor is not very sensitive to the variations in the structural and turbulence characteristics. In other words, for a wide range of structural and turbulence characteristics, the resonant MGLF component can be approximated by the resonant DGLF component, resulting usually in slightly conservative estimates of wind loads and associated responses.

DESIGN PROCEDURE

For design application, a simplified procedure for estimating the ESWL utilizing the MGLF is presented as follows:

- Step 1: Compute the mean wind force at each floor

$$\bar{P}_i = \left(\frac{1}{2} \rho \bar{U}_H^2 (Z_i/H)^{2\alpha} \right) C_D (W \cdot \Delta H_i) \quad (19)$$

where Z_i = height of the i th floor above the ground; and $\Delta H_i = Z_i - Z_{i-1}$.

- Step 2: Compute the mean BBM

$$\bar{M} = \sum_{i=1}^N \bar{P}_i Z_i \quad (20)$$

where N = number of floors of the structure.

- Step 3: Following the guideline of any current code or standard, obtain B , S , and E and compute the DGLF using a linear mode shape

$$G_{MB} = G_{YB} = 2g_u I_H \sqrt{B} \quad (21)$$

$$G_{MR} = G_{YR} = 2g_R I_H \sqrt{SE/\zeta} \quad (22)$$

$$G_M = 1 + \sqrt{G_{MB}^2 + G_{MR}^2} \quad (23)$$

- Step 4: Compute the resonant extreme BBM component

$$\hat{M}_R = G_{MR} \bar{M} \quad (24)$$

- Step 5: Compute the extreme ESWL at each floor. The resonant component can be obtained by distributing the BBM to each floor as a fraction of the extreme BBM according to

$$\hat{P}_{Ri} = \frac{m_i \varphi_i}{\sum m_i \varphi_i Z_i} \hat{M}_R \quad (25)$$

where $\varphi_i = \varphi_i(Z_i)$. Note that the distribution of the background ESWL is usually dependent on the response component under consideration and different from the mean and inertial components. Nevertheless, the following description serves as a fairly good approximation (Zhou et al. 1999a):

$$\hat{P}_{Bi} = G_{MB} \bar{P}_i \quad (26)$$

- Step 6: Estimate the extreme responses of interest through a simple static analysis. For example, the extreme displacement response can be computed simply by

$$\hat{Y}_i = G_M \bar{Y}_i \quad (27)$$

and the acceleration at each floor level is given by

$$\hat{a}_i = G_{MR} \cdot \bar{Y}_i \cdot (2\pi f_i)^2 \quad (28)$$

For other response components involving both the resonant and background contributions, e.g., the base shear and other internal forces, the resultant value can be obtained using an SRSS combination rule

$$\hat{r} = \bar{r} + \sqrt{(\hat{r}_B)^2 + (\hat{r}_R)^2} \quad (29)$$

where \bar{r} , r_B , and \hat{r}_R = mean, background, and resonant response components obtained from the static structural analysis by employing the above ESWL components separately. The resultant wind-induced response can then be combined with the response under the action of other loads.

NUMERICAL EXAMPLES

An example building with the following characteristics is used to illustrate the proposed scheme: $H \times W \times D = 200 \times 50 \times 40$ m; $f_1 = 0.22$ Hz; $\zeta = 0.01$; $\varphi_1(z) = (z/H)^\beta$; $m(z) = m_0[1 - \lambda(z/H)]$, $m_0 = 5.5 \times 10^5$ kg/m; $C_D = 1.3$. The wind environment is $\bar{U}_{10} = 30$ m/s; $\alpha = 0.15$; $\sigma_u/\bar{U}_{10} = 0.2$; and the

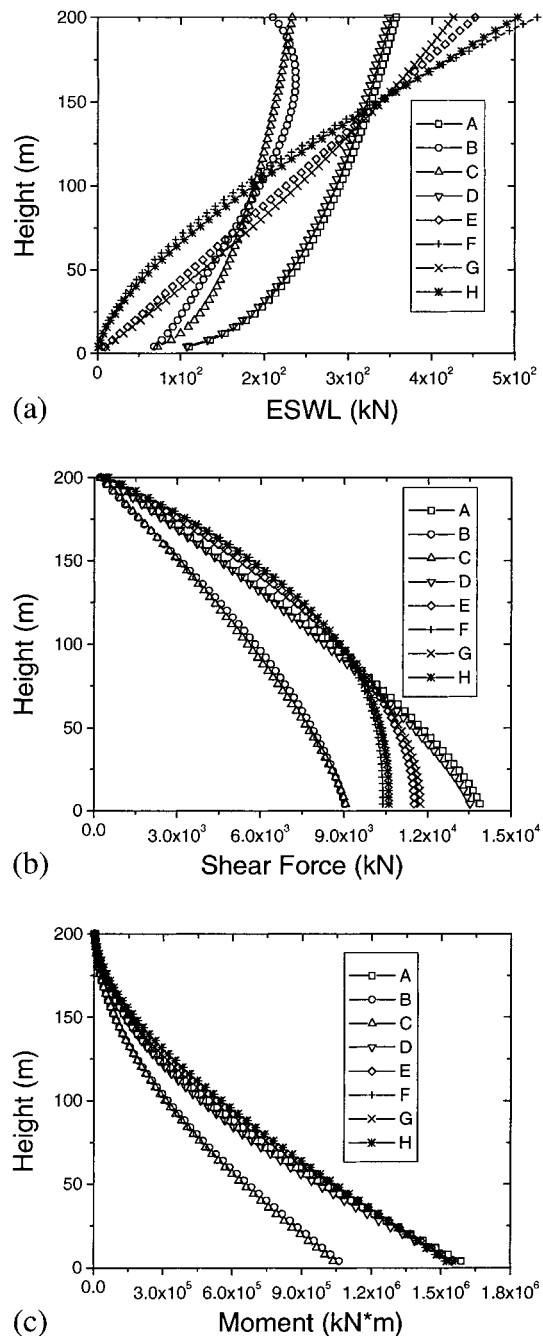


FIG. 3. Wind Loads/Effects Using DGLF and MGLF [A: Mean Wind Force; B: Background ESWL with Respect to BBM Response (Zhou et al. 1999a); C: Background ESWL by DGLF Approach; D: Resonant ESWL by DGLF Approach; E: Resonant ESWL by MGLF Procedure for Case 1; F: Resonant ESWL by MGLF for Case 2; G: Resonant ESWL by MGLF for Case 3; H: Resonant ESWL by MGLF for Case 4]

Davenport spectrum, $C_x = C_z = 11.5$. Four cases are considered here. In case 1, $\beta = 1.0$ and $\lambda = 0.0$; case 2, $\beta = 1.6$ and $\lambda = 0.0$; case 3, $\beta = 1.0$ and $\lambda = 0.2$; and in case 4, $\beta = 1.6$ and $\lambda = 0.2$.

The mean, background, and resonant ESWL components are separately computed using the DGLF method and the proposed MGLF procedure. These wind-loading components are plotted in Fig. 3.

The traditional DGLF method usually does not differentiate the cases that have nonlinear mode shapes or non-uniform mass, or both, from the case that has a linear mode shape and uniform mass, or case 1. Therefore, in the four cases studied here, the DGLF method gives the same result. The mean and

background ESWL components obtained using the MGLF procedure are the same as those obtained using the DGLF approach. However, the resonant component is different. Even for case 1, the ESWL given by the MGLF procedure has a linear distribution, which is clearly different from that given by the traditional method. The latter varies along the height following a 2α exponent law.

Due to the difference in the distribution of the wind loads, the estimated responses will be different. A comparison of different GLFs for different response components by the two procedures is given in Table 1. The items in brackets are the ratios between the GLFs obtained by the MGLF procedure and the corresponding GLFs obtained by the DGLF method. By definition, the DGLF method results in a uniform gust factor for all responses and for all four cases given here.

For case 1, the MGLF is, as expected, equal to the DGLF. A nonlinear mode shape (case 2), or a non-uniform mass (case 3), or both (case 4) influences the MGLF. However, as was exemplified in the preceding parameter study, the effect of the non-uniform mass is insignificant and the effect of a nonlinear mode shape is 2.2% on the resonant MGLF and 0.8% on the resultant MGLF, which are negligible. For case 4, the error is slightly reduced as compared with case 2.

The MGLF procedure determines the ESWL in a more realistic manner than the traditional DGLF method. Therefore, the resulting response estimates may differ. Using the base shear force as an example, the resonant base shear force by the MGLF procedure is 15% less than that obtained by the DGLF method for case 1, which resulted in a base shear gust factor that was 5.4% less than the DGLF. For case 2, the respective errors increase up to 23.2% and 8.3%. Although this effect is on the conservative side for the base shear force, this observation does not necessarily apply to other responses. Due to the difference in the distribution of the wind loading, the deviation in responses estimated by the DGLF method will depend on the response being estimated and the structural characteristics. For example, the resonant ESWL on the top floor obtained by the DGLF method is 33% ($350/520/\text{kN}$) less than the actual value, or the value given by the MGLF procedure for case 2.

The base shear GLF is more sensitive to the mode shape and mass distribution than the MGLF, and it is always different from the DGLF. In light of this sensitivity, the proposed procedure was not designed to use a base shear force to distribute the ESWL to floors, although this approach is used in earthquake engineering practice.

CONCLUDING REMARKS

The ESWL derived from the traditional DGLF method may deviate from the actual value, and consequently may lead to unfavorable estimates of some wind-induced load effects. This paper proposes a new procedure for determining the ESWL, which employs a BBM-based GLF or MGLF. The expected extreme BBM is computed by multiplying the mean BBM by the proposed MGLF. The extreme BBM is then distributed to all floors in a format very similar to the one used in earthquake engineering to distribute the base shear. In the case of linear structural mode shape, the proposed MGLF is numerically equal to the traditional DGLF. A parameter study suggests that, for cases in which the mode shape and the mass distributions depart from linear and uniform, respectively, a tacit assumption of equivalence between the MGLF and the DGLF would result in slightly conservative estimates of wind loading and associated response. This enables the use of the existing background information concerning DGLF in codes and standards in the proposed procedure.

The proposed MGLF scheme has several advantages over the DGLF approach. First, it provides the ESWL in a more

TABLE 1. Comparison of Gust Loading Factors

DGLF FORMULATION				MGLF FORMULATION					
All Responses				Base Bending Moment			Base Shear Force ^a		
Case (1)	G _B (2)	G _R (3)	G (4)	G _B (5)	G _R (6)	G (7)	G _B (8)	G _R (9)	G (10)
1	0.652	0.974	2.172	0.652 (1.000) ^b	0.976 (1.002)	2.174 (1.000)	0.652 (1.000)	0.829 (0.851)	2.055 (0.946)
2	0.652	0.974	2.172	0.652 (1.000)	0.953 (0.978)	2.155 (0.992)	0.652 (1.000)	0.748 (0.768)	1.992 (0.917)
3	0.652	0.974	2.172	0.652 (1.000)	0.976 (1.002)	2.174 (1.000)	0.652 (1.000)	0.845 (0.868)	2.067 (0.952)
4	0.652	0.974	2.172	0.652 (1.000)	0.959 (0.985)	2.160 (0.994)	0.652 (1.000)	0.763 (0.783)	2.004 (0.923)

^aGLF for base shear $G = \hat{Q}/\bar{Q}$ where peak base shear force, \hat{Q} , is computed using actual ESWLs, e.g., Eqs. (25) or (50) for resonant component; and \bar{Q} = mean base shear force.

^bItems in brackets are ratios between wind load effects obtained by MGLF formulation and those by DGLF formulation. These ratios are also equal to ratios of GLFs for wind effects of concern between these two GLF formulations. In DGLF, ESWL is determined by Eq. (1), while in MGLF it is by Eqs. (25) and (26).

realistic manner. This is the most important feature of the proposed procedure. Second, it uses the existing information, which permits a smooth transition from the DGLF to the MGLF formulation. Third, it is formulated in a format that is familiar to most design engineers. Fourth, a new analysis model, which is based on the BBM, is highlighted. In addition to its advantage in presenting the ESWL correctly, this model is relatively more straightforward than the current displacement-based model in ascertaining the aerodynamic admittance function (Zhou and Kareem, in preparation, 2000). Fifth, the application range has been extended to accommodate nonlinear mode shapes and non-uniform mass distributions. Sixth, it provides the opportunity for a generalized formulation and a consistent transition in prediction of response for structures ranging from relatively rigid to more flexible. Finally, it lays a foundation for the development of a consistent GLF model for 3D wind effects on tall buildings (Zhou and Kareem, in preparation, 2000). The base moment-based analysis and modeling also offers an attractive format for reducing wind tunnel data derived from HFBB and aeroelastic balance (Zhou and Kareem 2000).

APPENDIX I. DERIVATION OF DGLF

Usually, the mean structural displacement can be approximated well by the first mode mean displacement response

$$\bar{Y}(z) = \bar{P}_1^*/k_1^* \cdot \varphi_1(z) \tag{30}$$

where $\bar{P}_1^* = \int_0^H \bar{P}(z)\varphi_1(z) dz$, $k_1^* = (2\pi f_1)^2 m_1^*$, and $m_1^* = \int_0^H m(z)\varphi_1^2(z) dz$ = generalized load, stiffness, and mass of the first mode, respectively; f_1 = natural frequency of the first mode; the fundamental mode shape can be approximated by

$$\varphi_1(z) = c(z/H)^\beta \tag{31}$$

in which c and β = constants; and the mass is assumed to be linearly distributed as

$$m(z) = m_0(1 - \lambda(z/H)) \tag{32}$$

in which λ = mass reduction factor.

The fluctuating displacement can also be approximated with that in the first mode

$$\sigma_Y(z) = \left(\int_0^\infty S_{\xi_1}(f) df \right)^{1/2} \cdot \varphi_1(z) \tag{33}$$

where $S_{\xi_1}(f)$ = PSD of the fluctuating generalized displacement, which can be computed following the approach given by Davenport (1967) as shown in Fig. 1(a):

$$S_{\xi_1}(f) = \int_0^\infty S_u(f) \cdot \chi(\beta, f) \cdot |H_d(f)|^2 df \tag{34}$$

where $S_u(f)$ = PSD of the fluctuating wind velocity; χ = aerodynamic admittance function (not in the strict sense, similar to the mechanical admittance) that relates the wind velocity PSD to the PSD of the resulting fluctuating wind force, $S_{\bar{p}_1}(f)$. Using strip and quasi-steady theories and considering the wind structure in terms of vertical and horizontal correlations while ignoring the correlation between wind pressures on windward and leeward surfaces, the following relationship can be obtained:

$$S_{\bar{p}_1}(f) = \chi(\beta, f) \cdot S_u(f) \tag{35}$$

where

$$\chi(\beta, f) = \frac{(\rho C_D W H \bar{U}_H)^2}{(1 + \alpha + \beta)^2} \cdot |J_X(f)|^2 \cdot |J_Z(\alpha, \beta, f)|^2 \tag{36}$$

and

$$|J_X(f)|^2 = \frac{1}{W^2} \int_0^W \int_0^W R_X(x_1, x_2, f) dx_1 dx_2 \tag{37}$$

$$|J_Z(\alpha, \beta, f)|^2 = \frac{(1 + \alpha + \beta)^2}{H^2} \cdot \int_0^H \int_0^H \left(\frac{z_1}{H} \right)^{\alpha+\beta} \left(\frac{z_2}{H} \right)^{\alpha+\beta} R_Z(z_1, z_2, f) dz_1 dz_2 \tag{38}$$

are the joint acceptance functions in the horizontal and vertical directions, respectively; and

$$R_X(x_1, x_2, f) = \exp \left(- \frac{C_X f}{\bar{U}(h)} |x_1 - x_2| \right)$$

and

$$R_Z(z_1, z_2, f) = \exp \left(- \frac{C_Z f}{\bar{U}(h)} |z_1 - z_2| \right)$$

equal horizontal and vertical coherence functions of the fluctuating wind pressures, respectively. Also, C_X , C_Z = exponential decay coefficients; and h = reference height. Note that, based upon the formulation in Fig. 1(a) the aerodynamic admittance is the function of not only the turbulence characteristics and the architectural shape, but also the mode shape. The mechanical admittance function for the first mode displacement response is

$$|H_d(f)|^2 = |H_1(f)|^2 / k_1^{*2} \tag{39}$$

in which

$$|H_1(f)|^2 = \frac{1}{[1 - (f/f_1)^2]^2 + (2\zeta f/f_1)^2} \tag{40}$$

Using (3), (30), and (33), the fluctuating component of the DGLF can be computed by

$$\sigma_y(z)/\bar{Y}(z) = \left(\int_0^\infty S_{\bar{P}_1}(f) |H_1(f)|^2 df \right)^{1/2} / \bar{P}_1^* \quad (41)$$

which shows that the DGLF is independent of the mass.

To facilitate engineering computation, (41) is usually treated by dividing the integration into the background and resonant portions. The background and resonant components of the DGLF can be expressed, respectively, by

$$G_{YB} = 2g_u I_H \sqrt{B} \quad (42)$$

$$G_{YR} = 2g_R I_H \sqrt{R} \quad (43)$$

where $B = \int_0^\infty \kappa(\beta, f) S_u^*(f) df$ and $R = SE/\zeta =$ background and resonant response factors, respectively; $\kappa(\beta, f) = ((2 + 2\alpha)/(1 + \alpha + \beta))^2 \cdot |J_x(f)|^2 |J_z(\alpha, \beta, f)|^2$, which fulfills the function of the aerodynamic admittance; $S = \kappa(\beta, f) =$ size reduction factor; $E = (\pi f/4) S_u^*(f) =$ gust energy factor; $S_u^*(f) =$ normalized wind velocity spectrum with respect to the mean square fluctuating wind velocity, σ_u^2 ; and $I_H = \sigma_u / \bar{U}_H =$ turbulent intensity evaluated at the top of the structure. Most codes and standards use a linear mode shape assumption, or $\beta = 1$; and the DGLF components are then

$$G_{YB} = 2g_u I_H \frac{2 + 2\alpha}{2 + \alpha} \sqrt{\int_0^\infty |J_x(f)|^2 |J_z(\alpha, 1, f)|^2 S_u^*(f) df} \quad (44)$$

$$G_{YR} = 2g_R I_H \frac{2 + 2\alpha}{2 + \alpha} \sqrt{|J_x(f_1)|^2 |J_z(\alpha, 1, f_1)|^2 \cdot \frac{\pi f_1}{4\zeta} S_u^*(f_1)} \quad (45)$$

APPENDIX II. DERIVATION OF MGLF

The mean BBM on a building is given by

$$\bar{M} = \int_0^H \bar{P}(z)z dz = \frac{1/2 \rho C_D W \bar{U}_H^2 H^2}{2 + 2\alpha} \quad (46)$$

The fluctuating BBM response, like the displacement response, is evaluated in terms of the background and resonant components.

The background base moment can be derived following the expression in Davenport (1995) by employing the influence coefficient function $i(z) = z$:

$$\begin{aligned} \hat{M}_B &= g_u \sqrt{\left[\int_0^\infty \int_0^H \int_0^H \int_0^W \int_0^W (\rho C_D W \bar{U}_H)^2 \left(\frac{z_1}{H}\right)^\alpha \left(\frac{z_2}{H}\right)^\alpha \right. \\ &\quad \left. \cdot R_z(f) R_x(f) S_u(f) z_1 z_2 dx_1 dx_2 dz_1 dz_2 df \right]} \\ &= g_u \frac{I_H \rho \bar{U}_H^2 C_D W H^2}{2 + 2\alpha} \sqrt{\int_0^\infty S_u^*(f) |J_x(f)|^2 |J_z(\alpha, 1, f)|^2 df} \quad (47) \end{aligned}$$

When expressed in a nondimensional form, the background component of the MGLF is

$$G_{MB} = \frac{\hat{M}_B}{\bar{M}} = 2g_u I_H \frac{2 + 2\alpha}{2 + \alpha} \sqrt{\int_0^\infty S_u^*(f) |J_x(f)|^2 |J_z(\alpha, 1, f)|^2 df} \quad (48)$$

Since an influence function is used in (47), the contributions from the higher modes and mode coupling, which have been noted to be nonnegligible (Vickery 1995), have been automatically included.

On the other hand, for the resonant component, equivalent-static wind load is equal to inertial force. For a wind-excited structure, only the contribution of the resonant response in the first mode is typically considered. Using (31)–(36) and con-

sidering a nonlinear mode shape and a non-uniform mass distribution, the first mode extreme resonant displacement is given by

$$\begin{aligned} \hat{Y}_R(z) &= g_R \frac{(I_H \rho \bar{U}_H^2 C_D W)}{(2\pi f_1)^2 m_0} \frac{(1 + 2\beta)(2 + 2\beta)}{(1 + \alpha + \beta)[(2 + 2\beta) - \lambda(1 + 2\beta)]} \\ &\quad \times \sqrt{|J_x(f_1)|^2 \cdot |J_z(\alpha, \beta, f_1)|^2 \cdot \frac{\pi f_1}{4\zeta} S_u^*(f_1)} \cdot \left(\frac{z}{H}\right)^\beta \quad (49) \end{aligned}$$

Note that the displacement along the height follows the mode shape. The corresponding ESWL is given by

$$\begin{aligned} \hat{P}_R(z) &= (2\pi f_1)^2 m(z) \hat{Y}_R(z) = (g_R I_H \rho \bar{U}_H^2 C_D W) \\ &\quad \cdot \frac{(1 + 2\beta)(2 + 2\beta)}{(1 + \alpha + \beta)[(2 + 2\beta) - \lambda(1 + 2\beta)]} \\ &\quad \times \sqrt{|J_x(f_1)|^2 \cdot |J_z(\alpha, \beta, f_1)|^2 \cdot \frac{\pi f_1}{4\zeta} S_u^*(f_1)} \cdot \left(1 - \lambda \frac{z}{H}\right) \left(\frac{z}{H}\right)^\beta \quad (50) \end{aligned}$$

It can be observed that the distribution of the ESWL is related to the mode shape and the mass distribution. The BBM induced by the load in (50) can be derived by

$$\begin{aligned} \hat{M}_R &= \int_0^H \hat{P}_R(z)z dz = (g_R I_H \rho \bar{U}_H^2 C_D W H^2) \\ &\quad \cdot \frac{(1 + 2\beta)(2 + 2\beta)}{(1 + \alpha + \beta)[(2 + 2\beta) - \lambda(1 + 2\beta)]} \frac{[(3 + \beta) - \lambda(2 + \beta)]}{(3 + \beta)(2 + \beta)} \\ &\quad \times \sqrt{|J_x(f_1)|^2 \cdot |J_z(\alpha, \beta, f_1)|^2 \cdot \frac{\pi f_1}{4\zeta} S_u^*(f_1)} \quad (51) \end{aligned}$$

Rewriting in a nondimensional form, the resonant component of the MGLF is

$$\begin{aligned} G_{MR} &= \frac{\hat{M}_R}{\bar{M}} = 2g_R I_H \frac{(1 + 2\beta)(2 + 2\beta)(2 + 2\alpha)}{(1 + \alpha + \beta)[(2 + 2\beta) - \lambda(1 + 2\beta)]} \\ &\quad \cdot \frac{[(3 + \beta) - \lambda(2 + \beta)]}{(3 + \beta)(2 + \beta)} \times \sqrt{|J_x(f_1)|^2 \cdot |J_z(\alpha, \beta, f_1)|^2 \cdot \frac{\pi f_1}{4\zeta} S_u^*(f_1)} \quad (52) \end{aligned}$$

ACKNOWLEDGMENT

The writers gratefully acknowledge the partial support from NSF Grants CMS 95-03779 and CMS 95-22145 for this study.

APPENDIX III. REFERENCES

- American Concrete Institute (ACI). (1988). "Standard practice for the design and construction of cast-in-place reinforced concrete chimneys." *ACI 307-88*, Detroit.
- Architectural Institute of Japan (AIJ). (1996). "Recommendations for loads on buildings." Tokyo.
- ASCE. (1999). "Minimum design loads for buildings and other structures." *ASCE 7-98*, 9, Reston, Va.
- Australian Standards. (1989). "SAA Loading code, part 2: Wind forces." *AS1170.2-89*, Australia.
- Boggs, D. W. (1991). "Wind loading and response of tall structures using aerodynamic models." PhD thesis, Colorado State University, Fort Collins, Colo.
- Boggs, D. W., and Peterka, J. A. (1989). "Aerodynamic model tests of tall buildings." *J. Engrg. Mech.*, ASCE, 115(3), 618–635.
- Davenport, A. G. (1967). "Gust loading factors." *J. Struct. Div.*, ASCE, 93(3), 11–34.
- Davenport, A. G. (1999). "Missing links in wind engineering." *Proc., 10th ICWE*, Copenhagen, 1–8.
- Drybre, C., and Hansen, S. O. (1997). *Wind loads on structures*, Wiley, New York.

- “EUROCODE 1: Basis of design and actions on structures, part 2.4: Actions on structures—wind actions.” (1995). *European Prestandard ENV 1991-2-4*.
- Kareem, A. (1986). “Synthesis of fluctuating along-wind loads on tall buildings.” *J. Engrg. Mech.*, ASCE, 112(1), 121–125.
- Lee, B. E., and Ng, W. K. (1988). “Comparisons of estimated dynamic along-wind responses.” *J. Wind Engrg. Indust. Aerodyn.*, 30, 153–162.
- National Research Council of Canada (NRCC). (1996). “User’s guide—NBCC1995 structural commentaries (part 4).”
- Simiu, E., and Scanlan, R. (1996). *Wind effects on structures: fundamentals and applications to design*, 3rd Ed., Wiley, New York.
- Solari, G. (1993a). “Gust buffeting. I: Peak wind velocity and equivalent pressure.” *J. Struct. Engrg.*, ASCE, 119(2), 365–382.
- Solari, G. (1993b). “Gust buffeting. II: Dynamic along-wind response.” *J. Struct. Engrg.*, ASCE, 119(2), 383–397.
- Solari, G., and Kareem, A. (1998). “On the formulation of ASCE 7-95 gust effect factor.” *J. Wind Engrg. Indust. Aerodyn.*, 77–78, 673–684.
- Vickery, B. J. (1995). “The response of chimneys and tower-like structures to wind loading.” *Proc., 9th Int. Conf. on Wind Engrg.*, New Delhi, 205–233.
- Zhou, Y., Gu, M., and Xiang, H. F. (1999a). “Along-wind static equivalent wind loads and response of tall buildings. I: Unfavorable distributions of static equivalent wind loads.” *J. Wind Engrg. Indust. Aerodyn.*, 79(1–2), 135–150.
- Zhou, Y., Gu, M., and Xiang, H. F. (1999b). “Along-wind static equivalent wind loads and response of tall buildings. II: Effects of the mode shape.” *J. Wind Engrg. Indust. Aerodyn.*, 79(1–2), 151–158.
- Zhou, Y., and Kareem, A. (2000). “Aeroelastic balance.” *Proc., 4th Int. Colloquium on Bluff Body Aerodyn. and Applications*, Bochum, Germany, 599–602.
- Zhou, Y., Kareem, A., and Gu, M. (1999c). “Gust loading factors for design applications.” *Proc., 10th ICWE*, Copenhagen, 169–176.
- Zhou, Y., Kareem, A., and Gu, M. (2000). “Equivalent static buffeting wind loads on structures.” *J. Struct. Engrg.*, ASCE, 126(8), 989–992.